The International Journal of Advanced Manufacturing Technology (2023) 128:5117–5127
https://doi.org/10.1007/s00170-023-12199-y

ORIGINAL ARTICLE

Grain refinement of aluminium welds by Ti, TiB_2, and TiC filler wire inoculation

Kjell Martin Kirkbakk[1] · Nikolai Marhaug[2] · Geir Kvam-Langelandsvik[2] · Jens Christofer Werenskiold[1]

Received: 13 April 2023 / Accepted: 19 August 2023 / Published online: 5 September 2023

Abstract
A fine-grained fusion zone characterises a tough aluminium weld. To improve the solidification characteristics and refine the grains in aluminium welding, different inoculation particle combinations were introduced to the filler wire by solid state metal screw extrusion. Filler wires were I-joint welded with two different welding methods to reveal the potency for grain refinement. Grain size, microstructure, porosity content, and hardness across the weld was revealed. Gas metal arc welding with a Ti-TiC inoculated filler wire exhibited a remarkable grain refinement of 91% compared to a base reference of commercial pure aluminium. The Al_3Ti intermetallic phase was found as nucleation point. Gas tungsten arc welding showed lower grain refinement potency, and no Al_3Ti phase was found in any weld. Thus, the effect of welding method must be taken into consideration upon development of inoculant containing filler wires.

Keywords GMAW · GTAW · Welding · Inoculation

1 Introduction

Arc welding is one of the most important joining techniques for metals [1, 2]. High productivity and metallurgical bonding make it the preferred joining solution for a range of applications. However, joining of aluminium and its alloys has been deemed challenging. One of the main issues at present is local softening in vicinity of the fusion zone, i.e., the heat affected zone (HAZ). This effect is seen due to annihilation of dislocations or over-aging of strengthening precipitates. Consequently, design standards impose up to a 50% yield strength penalty of aluminium when welding is used as joining method [3]. For light-weight structures in the automotive and offshore sectors, overcoming this strength penalty is of paramount importance.

One solution to compensate the strength loss is to protect the weak HAZ. This can possibly be achieved by combining a narrow HAZ and a higher strength of the weld metal compared to the base material, i.e., weld zone overmatch. The deformation can then be transferred from the HAZ to the base metal. Weld zone overmatch conditions require a filler wire with high strength in the as-welded state. However, today's market only supply non-heat treatable filler wires with intermediate strength [4]. High strength heat-treatable filler wires are currently not available due to the high susceptibility to solidification cracking in the fusion zone. This issue can be overcome by promoting growth of equiaxed grains through inoculation. Janaki Ram et al. [5] compared additions of Ti-B and Ti to a 7020 aluminium alloy by gas tungsten arc welding (GTAW) welding. Ti-B additions were particularly efficient to refine grains in the fusion zone and reduce the cracking susceptibility. Similar effects has been found with Ti-B master alloys for aluminium alloys like 2090, 6082, and 7055 [6–9]. Similarly, introduction of TiC nanoparticles to the filler wire has shown a remarkable effect as grain refiner and increase the weld metal strength. Fattahi et al. [10] manufactured GTAW strips by accumulated roll bonding, creating a well-dispersed wire with excellent mechanical properties after welding. Sokoluk et al. [11] developed an innovative

✉ Geir Kvam-Langelandsvik
geir.langelandsvik@sintef.no

Nikolai Marhaug
nikolai.marhaug@sintef.no

Jens Christofer Werenskiold
jens.c.werenskiold@ntnu.no

[1] Department of Materials Science and Engineering, NTNU Norwegian University of Science and Technology, Trondheim 7491, Norway

[2] SINTEF Industry, Richard Birkelands vei 2B, Trondheim 7034, Norway

flux-assisted casting method to incorporate TiC nanoparticles into aluminium, resulting in a fine-dispersed Al-TiC composite after welding. Although there exist numerous studies regarding grain refinement in welding, the inoculation mechanisms have not been studied in detail. The isolated effect of titanium particles on grain refinement in welding is also scarcely reported. Furthermore, it is noteworthy that all mentioned studies have been performed with GTAW. These results are not directly transferable to other welding methods, such as gas metal arc welding (GMAW), and need further examination.

Welding filler wires are primary manufactured by a liquid state process, i.e., casting. Inoculant particles are prone to fading, agglomeration, and settlement during the smelting process, thus decreasing their grain refinement potency [12]. When remelted during fusion welding, inoculants risk being faded and not provide sufficient grain refinement [13]. This is especially relevant for nanoparticle sized particles. An alternative solution to casting is in situ mixing of aluminium and inoculant particles during solid state processing. Metal screw extrusion has shown promising results for filler wire production [14] and will further be elucidated in this study.

GTAW utilises a non-consumable tungsten electrode to establish an electric arc that melts the workpiece to form a melt pool. It is important to note that the tungsten electrode does not melt and that the filler wire must be added from outside the arc. For most metals, the conventional setup is to use direct current (DC) with the electrode connected to the negative pole of the power supply, i.e., direct current electrode negative (DCEN). However, as is well known, aluminium and its alloys have a fast forming Al_2O_3 oxide layer with a melting temperature of 2060 °C. This film must be broken down in order to avoid weld defects such as lack of fusion and oxide entrapment. For other gas shielding arc welding methods (e.g., GMAW), this can be done with a direct current positive electrode (DCEP), as the resulting ion bombardment will disperse the oxide film. However, this setup is not optimal for GTAW as it generates too much heat on the tungsten electrode. A common workaround is to use alternating current (AC) instead, as the electrode will cool on the negative half-cycle and disperse the oxide film on the positive half-cycle. Note that the current is constant with the GTAW method, while the voltage varies slightly depending on the momentary arc length [15]. Overall, the GTAW method is very well suited for welding thin structures due to its stable arc at low welding currents. It is less used for welding thicknesses above 6 mm due to its low filler metal deposition rate and slow welding speeds.

GMAW is fundamentally different to GTAW in that the filler wire also acts as the electrode. During welding, the spooled wire is continuously fed by a drive unit through the welding torch. As the filler wire passes the contact tube, it becomes connected to the power source and short circuits on contact with the workpiece. This creates an electric arc that melts both the filler wire and the base metal and establishes a weld pool. It is most common to use DCEP in welding of aluminium and its alloys, as this setup results in a very good dispersion of the oxide film. Furthermore, it is the voltage that is normally kept constant during GMAW, as opposed to the current-locked GTAW. This is because a constant voltage aid to maintain a stable arc length. It is important to note that GMAW can transfer the filler wire to the weld pool in two different ways, i.e., dip transfer and spray transfer. During dip transfer, which normally takes place at low welding currents, the wire is not melted fast enough to maintain an arc above the weld pool. Thus, the wire is "dipped" into the weld pool where it short circuits, before being drawn into the weld pool by surface tension effects. During spray transfer, the filler wire is melted in the arc above the weld pool, which causes smaller droplets of the wire to be sprayed across the weld pool. Compared to dip transfer, spray transfer usually results in deeper penetration and less spatter. Due to the low melting point of aluminium, spray transfer can generally take place at lower currents compared to other metals. However, a fairly recent process called pulsed GMAW has made it possible to achieve spray transfer at lower (average) currents. This process utilises a background current that barely maintains the arc without melting the filler wire. A high frequency peak of higher current is then superimposed, which causes a single droplet of filler wire to spray transfer. Due to the high welding speed, the HAZ of GMAW is usually smaller compared to GTAW. Furthermore, the deposition rate of GMAW is usually higher, and the method is considered easier to use in all positions as the welder does not have to control the wire feed rate manually.

The aim of this study is to evaluate the grain refining efficiency of different inoculants in metal screw extruded filler wires, derive the nucleation mechanisms, and determine the influence of two joining techniques (i.e., GMAW and GTAW) on weld structure properties.

2 Materials and methods

2.1 Filler wire production

A total of four inoculated filler wires were produced by metal screw extrusion, each with different particle additions of Ti (diameter 150 µm), TiB_2 (500 nm), and TiC (40–60 nm) according to Table 1. One filler wire without additions was also produced as reference. A commercial pure AA1370 aluminium alloy was chosen as base material for the filler wires. This was done to reduce the complexity and better highlight the effects of each particle combination. The chemical composition of AA1370 is given in Table 2.

Table 1 Filler wires produced by metal screw extrusion

Filler wire	Base alloy	Particle addition (wt.%)	Particle size (μm)
Al-ref	AA1370	–	–
Al-Ti	AA1370	1.5 Ti	150
Al-Ti-TiB_2	AA1370	1.5 Ti, 0.25 TiB_2	150, 0.5
Al-TiC	AA1370	2 TiC	0.05
Al-Ti-TiC	AA1370	1.5 Ti, 2 TiC	150, 0.05

AA1370 in the form of granules and particles as dry powder was roll mixed in inert Ar atmosphere for 48 h. In this way, the aluminium granules obtained a thin particle coating. The particle-coated aluminium was compacted and extruded by a laboratory metal screw extruder. The extrusion procedure has been outlined by Langelandsvik et al. [14]. Particle-air-moisture interactions are supposed to contaminate the material prior and during screw extrusion. The extrusion system was therefore insulated and flushed with argon gas during the experiments to avoid air exposure of the materials. Ø3 mm wires were screw extruded with an even dispersion of particles in the aluminium matrix. Extrusion temperature was 500 °C. Wires were subsequently cold drawn to Ø1.6 mm. To avoid contamination from surface hydrocarbons and moisture during welding, wires were cleaned in an ultrasonic acetone bath and stored in a heating cabinet of 50 °C until the day of welding.

2.2 Welding

Arc welding was performed on AA1050-H14 sheets (dimensions 300 × 100 × 3 mm^3) with composition as shown in Table 2. Sheets were clamped together over a stainless steel backing, forming a gap-less I-joint butt weld. The aluminium oxide layer was mechanically removed by a stainless steel brush and cleaned with acetone. Ten weld coupons were produced, utilising five filler wires and two welding methods, i.e., GMAW and GTAW. The welded joints are shown in Fig. 1, as well as micrographs of the filler wire surface.

In GMAW, the filler wire serves as the electrode and was conducted with a Fronius 400i pulsed power source. The power source was connected to an ABB IRB2400 six degrees of freedom manipulator who provided an even welding speed of 10 mm/s. Contact tip to work distance was set to 12 mm, travel angle was 6° pushing, and shielding gas flow rate was 20 L/min of 99.999% Ar. The welding parameters were equal for all coupons as shown in Table 3.

In GTAW, the filler wire is supplied to the arc from a non-consumable electrode and was performed manually using a Migatronic 2500 power source with Ø2.4 mm tungsten electrode (Migatronic SuperBlue). GTAW require thicker filler wires than GMAW; hence, three Ø1.6 mm wires were twinned. Due to the manual operation of GTAW, the welding parameters were not constant for all coupons. A dummy coupon was conducted for all filler wires to obtain optimum welding parameters. Some fluctuations in arc voltage (±1 V) were observed due to fluctuating arc length during welding. An approximate arc voltage was measured by a voltmeter with probes between the negative ground clamp and the positive pole at the power source. Average welding speed was determined by measuring the total weld time for each coupon. The shielding gas flow rate was 20 L/min of 99.999% Ar. An overview of the GTAW welding parameters is given in Table 3. The supplied arc energy AE in all experiments has been calculated through the relation $AE = IU/v$ with current I (A), voltage U (V), and welding torch speed v (mm/s) as input. As seen in Table 3, GTAW supplies more energy to the workpiece than GMAW.

2.3 Characterisation

Weld coupons were examined in terms of microstructure and mechanical properties. Materials were prepared for microstructural examination by mechanical grinding with water-lubricated SiC discs and polishing with water-based diamond suspension. Colloidal silica dispersion with diameter 0.04 μm was used at the final stage to obtain a scratch- and deformation-free surface. All welds were examined in transverse cross section. Area fraction porosity in the solidified weld was determined by optical microscopy. Three sections of each weld were examined, and porosity was quantified by the open-source software ImageJ. Grain structure was examined on samples anodised in Barkers' reagent (5 mL HBF_4, 95 mL H_2O) under cross-polarised light with a sub-lambda

Table 2 Element composition in wt.% of base filler wire and base welding plate

Alloy	Fe	Si	Ga	Ni	Cu	Mn	Mg	Zn	Ti	Al
AA1370	0.12	0.04	0.01	–	–	–	–	–	–	Bal
AA1050-H14	0.32	0.06	–	–	0.001	0.002	–	0.002	0.017	Bal

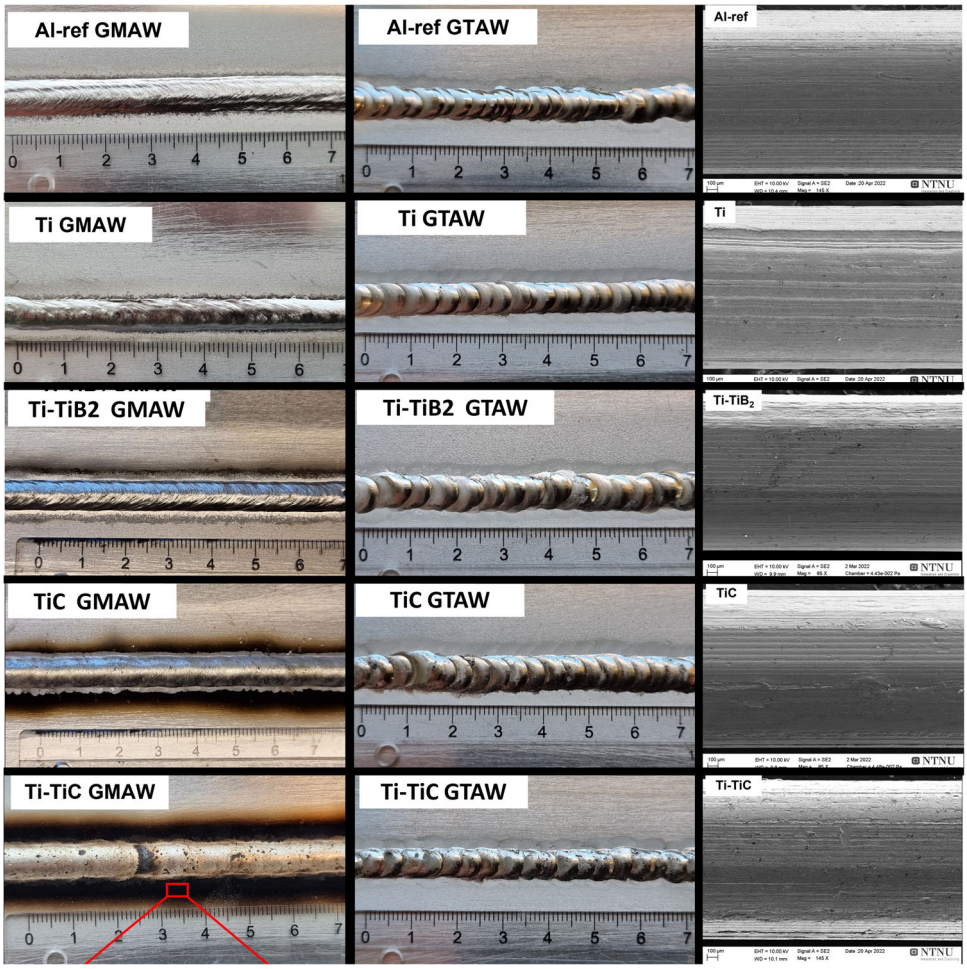

Fig. 1 Welded joints with different filler wires. SEM micrographs of wires are depicted to the right, showing adequate surface quality

plate inserted in the column. Mean grain size was determined by the circular intercept method according to ASTM E112-13 [16]. In-depth analyses of particles and microstructure were performed with scanning electron microscopy. Backscatter electron signal coupled with energy dispersive X-ray spectroscopy (EDX) was used to qualitatively determine phase compositions.

Mechanical assessment was performed by Vickers microhardness. Due to the elevated porosity level in some welds, a low impact load of 100 g was used ($HV_{0.1}$). Hardness was reported as a profile starting at the weld centerline and reaching 20 mm horizontally on each side. Thus, the hardness of the weld metal, HAZ, and unaffected base material could be evaluated. The distance between each indent was 1 mm according to ISO 6507-1 [17].

3 Results and discussion

3.1 Grain refinement

Commercial pure aluminium possesses a low amount of solute that restricts the growing solidification front by partitioning. Combined with few and impotent nucleation sites, the final grain size of commercial pure aluminium is expected

Table 3 Welding parameters for I-joint welding without air gap

Parameter	GMAW	GTAW				
	All	Al-ref	Ti	Ti-TiB_2	TiC	Ti-TiC
Current (A)	120	135	135	135	140	130
Voltage (V)	18	11	11	11	12	11
Welding speed (mm/s)	10	2	3	2	3	3
Arc energy (kJ/mm)	0.22	0.74	0.50	0.74	0.56	0.48

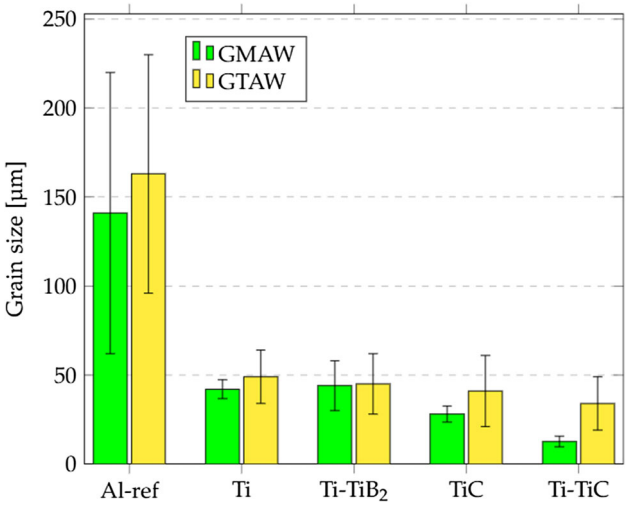

Fig. 2 Grain size in the fusion zone with different filler wires and welding methods

to be large after welding. This is indeed the case as seen in Fig. 2, where the mean grain size of the Al-ref filler wire is over 100 µm in diameter, regardless of welding method. Addition of inoculation particles to the filler wire changes this situation drastically. A $69-91\%$ and $70-79\%$ decrease in average grain size was observed for materials welded with GMAW and GTAW, respectively. GMA welds have overall a finer grain structure compared to respective materials joined by GTAW. This can be attributed to the supplied heat input which is higher for GTAW. The elevated heat input decreases the cooling rate of the fusion zone, leading to increased time for grain growth during solidification for GTA welds.

A higher partitioning of solute is partly responsible for the observed grain refinement. Titanium is known to be one of the most efficient grain growth restricting elements for aluminium [18]. Significant Ti additions increase the constitutional undercooling and is thus the driving force for nucleation. Solute titanium is therefore an efficient measure for grain refinement. This is evident by examination from Fig. 3, where addition of titanium microparticles to the wire chemistry significantly refined the grain size after welding for both GMAW and GTAW. However, solute titanium is not necessarily efficient in itself to alter the grain morphology from columnar to equiaxed. The grain structure for all welded joints in Fig. 3 shows that additions of titanium alone creates a significant portion of columnar grains towards the fusion line between the fusion zone and unmelted base material. A potent nucleation point is therefore necessary to fully utilise the excess solute present in the melt. TiC in combination with solute Ti was the most efficient grain refinement combination observed, with a fully equiaxed grain structure in GMAW and

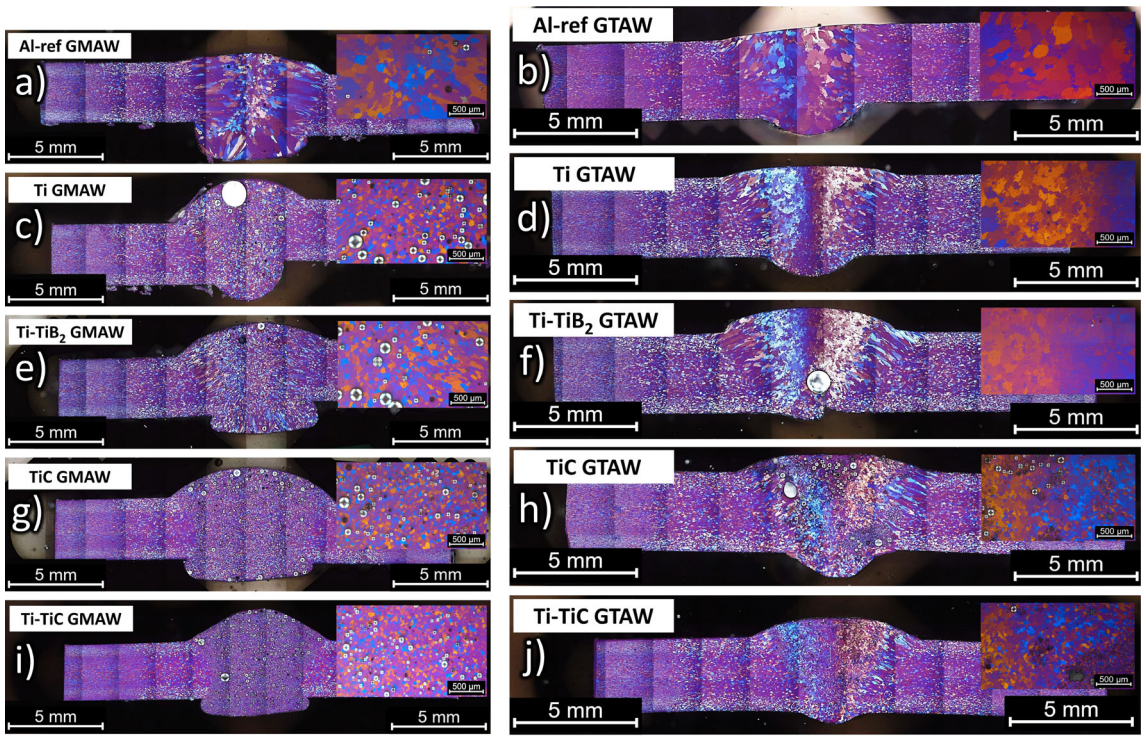

(a) GMAW (b) GTAW

Fig. 3 Grain structures of produced welds in cross section under polarised light. Micrographs of each weld in the centerline are included to the upper right of each image

an almost fully equiaxed structure in GTAW. As opposed to several other works, a Ti-TiB_2 particle mixture do not seem to improve the grain refinement potency [8, 9, 19]. In fact, Ti additions alone is similar or even more efficient compared to a combined Ti-TiB_2 mixture. The nucleation mechanisms of the investigated materials are examined further in the following section.

3.2 Microstructure and nucleation

Microstructural details observed in the weld fusion zone of different materials are summarised in Fig. 4. All materials possess primary particles from trace iron and silicon precipitated as Al-Fe and Al-Fe-Si intermetallics, mostly situated at grain boundaries. Such particles appear bright in backscatter SEM due to a higher mean atomic number than aluminium. Primary particles are not indicated in Fig. 4. Materials joined by GMAW are shown in Fig. 4a, c, e, and g. When Ti alone is mixed into the filler wire, it is dissolved and re-precipitated as $TiAl_3$ intermetallics during GMAW, evidenced by EDX measurements [20]. The weld fusion zone has a hyperperitectic composition (>0.15 wt.% Ti) when accounting for base metal dilution. Titanium is thus supersaturated in the melt and produce fine intermetallics during solidification. It has been stated by Zhang et al. [21] that $TiAl_3$ is one of the most potent nucleation sites for α-aluminium due to the close-to-perfect lattice match. The highly efficient grain refinement can therefore be ascribed the precipitation of fine

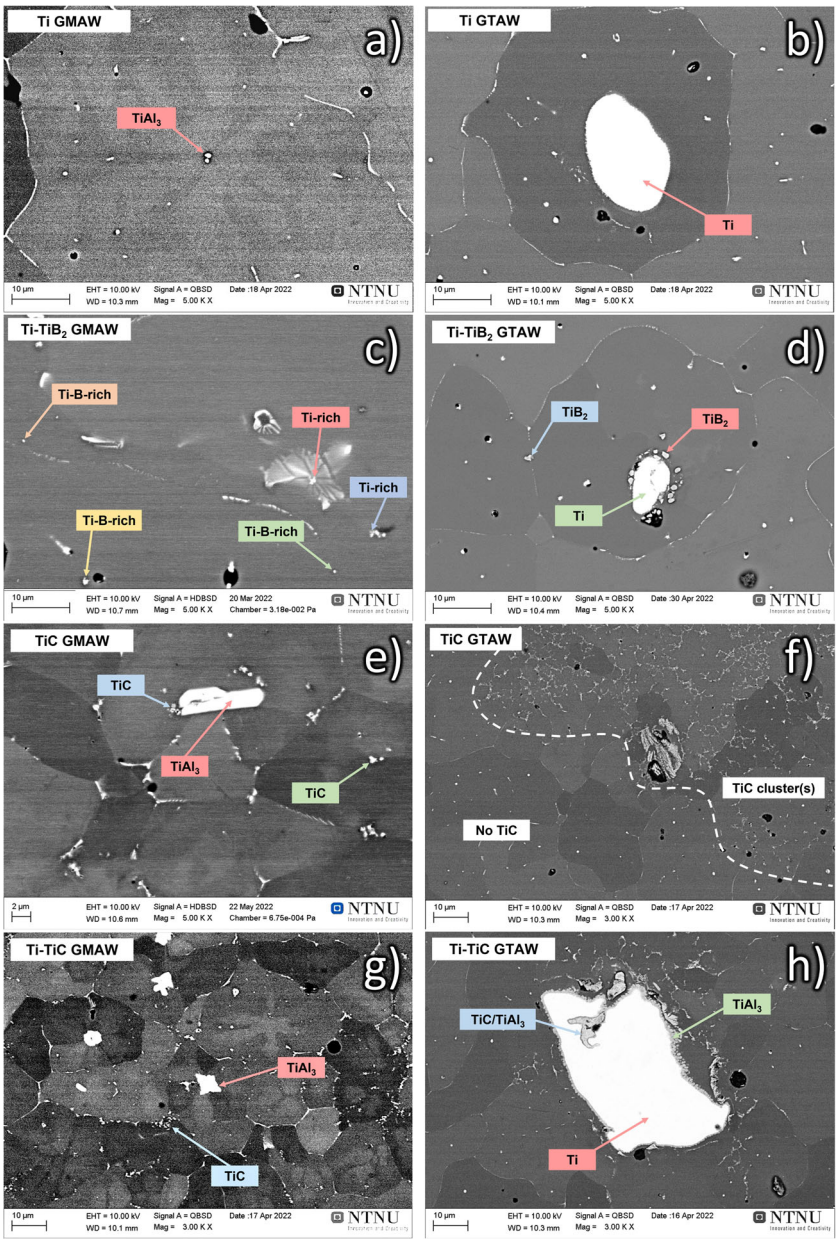

Fig. 4 SEM backscatter micrographs in inoculated weld fusion zones

$TiAl_3$ intermetallics. A petal-like structure radiating from the nucleation site was observed, as seen in Fig. 4a and g. Due to the brighter appearance of the structure, it is of a higher atomic number than aluminium, and EDX line scans indicate an enrichment of titanium. The congestion of solute titanium around a nucleation point is in line with the *Ti transition zone theory* proposed by Yu and Liu [22].

GTAW of the Al-Ti filler wire was unable to fully dissolve the relatively large Ti particles of 10–50 μm in diameter. As seen in Fig. 4b, a pure titanium particle is partly dissolved to a size of <10 μm with rounded edges. Consequently, less titanium is introduced to the melt resulting in a hypoperitectic composition. It is therefore less likely to obtain precipitation of $TiAl_3$ inoculants. Nucleation in these welds were observed to originate from rather impotent ferrous intermetallics or sporadically on large titanium particles.

Additions of TiB_2 seemed to be rather impotent as to refine the fusion zone microstructure. For the GMA weld in Fig. 4c, titanium-boron rich particles (exact composition could not be determined) were mainly observed on grain boundaries, indicating a rather insignificant effect as nucleation site. The Ti-B particles were smaller compared to the original particle size (Table 1), indicating that the fusion heat in the arc had influenced the morphology and possibly the composition. The $TiAl_3$ phase was observed as a likely grain refining phase. In GTAW, particles with close composition to TiB_2 were found on grain boundaries and agglomerated to Ti particles (Fig. 4d). Their size and morphology seemed rather unaffected post welding.

An apparent lack of grain refining effect from the TiB_2 particles in this work contradicts several studies reporting a significant grain refining effect of TiB_2 in GTAW [5–7, 23]. The particle characteristics of TiB_2 in this work could possibly explain the observed discrepancy. Previous studies have utilised Al-Ti-B master alloys to produce the filler material by casting, but the actual presence of TiB_2 particles in the produced filler wire was never documented. It is possible that the presumed TiB_2 particles produced in the casting process have been coated by a layer of $TiAl_3$, fulfilling the requirements for efficient grain refinement related to the *duplex nucleation theory* [24]. The present study with solid-state processing and rapid fusion and solidification during welding is possibly insufficient to create a $TiAl_3$ layer on the TiB_2 particles, making the particles impotent for nucleation of α-grains.

Addition of TiC nanoparticles produced the finest microstructures irrespective of welding method. Combined with elemental titanium, fine grains with diameter of 13±3 μm were produced by GMAW (Fig. 4g). It is evident that a fraction of the TiC nanoparticles are dissolved during GMAW and precipitated as $TiAl_3$ working as nucleation sites. Titanium petal-formed enrichment is observed in grain centres. Remaining TiC are settled on grain boundaries, where they work as grain growth inhibitors [25]. Nanoparticles are therefore inefficient as nuclei for grain refinement, in agreement with the *free growth model* by Greer et al. [26]. GTAW of the Ti-TiC filler wire exhibited particle accumulation at certain areas, with partly melted titanium particles surrounded by TiC nanoparticles. The nanoparticle survivability in GTAW was profound compared to GMAW.

$TiAl_3$ is the dominating nucleation phase in all materials joined by GMAW. The micron-sized titanium particles is fully dissolved in all GMA welds, and a petal-shaped titanium enrichment was frequently observed surrounding $TiAl_3$. This observation is in opposition to the statement of Dvornak et al. [27] which claims that the cooling rates in welding are too high for $TiAl_3$ precipitation, even for hyperperitectic compositions. It seems plausible that $TiAl_3$ is formed due to supersaturation of elemental Ti in the material.

For filler wires with sole additions of TiC, heterogeneous nucleation was found on the $TiAl_3$ phase as well. A likely cause is dissolution of TiC into $TiAl_3$ and Al_4C_3 [28]. Thus, a fraction of the TiC (and TiB_2) nanoparticles do not survive the thermal cycle involved in GMAW. This holds true for titanium microparticles as well, which are fully dissolved in the weld metal. The reason for this is related to the thermal history of the filler wire in GMAW. The filler wire works as the electrode in GMA welding and is melted high up in the electric arc before travelling to the workpiece in spray mode. The filler wire is therefore subjected to very high temperatures, possibly reaching 15,000–20,000 K for a short period of time [29, 30]. The weld pool has therefore a composition which is highly potent for nucleation, which promotes a fine microstructure after solidification. Combined with the relatively fast cooling rate due to the lower arc energy transmitted to the workpiece, the microstructure becomes very fine.

Filler wires deposited by GTAW possess different microstructural characteristics compared to the GMAW counterpart. The most prominent difference is the survivability of Ti, TiB_2, and TiC particles. In the TiC GTAW weld, no $TiAl_3$ was observed in the structure. Micron-sized Ti particles were hence only partly dissolved during welding. These observations are not in line with the supplied heat input to the workpiece, which is higher for GTAW compared to GMAW. The explanation is related to the filler wire feeding scheme in GTAW. The filler wire is fed at the front of the electric arc, thus not subjected to the hottest part of the arc. The peak temperature of the filler wire is therefore well below 10,000 K [31], which ensure that the ceramic TiB_2 and TiC particles remain their size, morphology, and composition. Thus, the welding method has a decisive role of the final microstructure of a fusion weld.

3.3 Porosity

The average area fraction porosity in three different sections of each weld is presented in Fig. 5. The pure reference

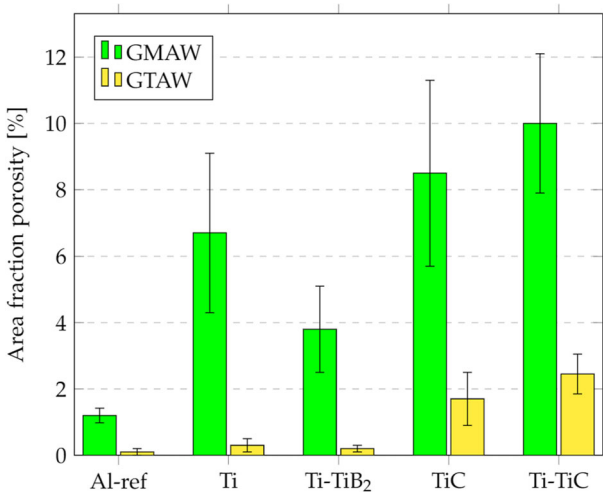

Fig. 5 Porosity content in examined materials

filler wire Al-ref fused by GMAW exhibited a relatively low amount of porosity. GTAW with the reference wire resulted in an almost pore free weld. This is an indication that the metal screw extrusion process itself produce filler wires with sufficient quality to be used for arc welding.

Furthermore, it is clear that GMAW provides an elevated porosity content, especially concerning materials mixed with inoculant particles. The highest area porosity of 10±2% was observed for the most fine-grained weld using the Ti-TiC filler wire. Large pores were generally observed close to weld edges [20]. The gas escape in GMAW is restricted due to high welding speeds and rapid solidification, combined with restricted gas escape through the aluminium oxide surface skin due to surface tension [32]. GTAW supplies more heat input to the work piece which enables gas escape, which in turn decrease the final porosity content.

Turbulence in the melt pool can further lead to excessive porosity formation [33]. The spray transfer mode in pulsed GMAW induce more turbulence and spatter compared to dip transfer modes (e.g., GTAW and cold metal transfer). As the drawn wire was spooled manually, the wire feeding into the melt pool was likely erratic, further increasing the turbulence and an unstable arc. Spooling issues are not present in GTAW as the wire is manually fed into the melt pool.

TiC nanoparticle additions to the filler wire increased the pore content significantly. It is well known that the most common porosity source in aluminium welds stem from hydrogen, which has a large liquid–solid solubility difference [34]. Contamination sources includes the base material and filler wire through hydrocarbons, moisture, and hydrated surface oxides. The base materials was ground and cleaned prior welding, thus being an unlikely contamination source. The ceramic powder component mixed into the filler wires (i.e., Ti, TiB_2, and TiC) may introduce hydrogen into the material. TiC nanoparticles are believed to be highly reactive towards air and humidity, possibly picking up moisture from ambient atmosphere [28, 35]. Although material preparation and screw extrusion of Al-TiC materials were performed under argon gas shielding, air contamination can not be excluded. The most efficient measure to avoid porosity in the produced welds is therefore to restrict the hydrogen content in the filler wires. It could also be postulated that TiC dissolves to $TiAl_3$ intermetallics and CO/CO_2 gas during welding. However, the strong affinity of aluminium to oxygen ($\Delta G^\circ = -1582$ kJ/mol) render this claim thermodynamically impossible. Given the fact that filler wires of the same batch resulted in very different porosity levels for GMAW and GTAW, it is shown that the welding method is highly relevant for the final porosity content.

3.4 Mechanical properties

Hardness profiles of all produced welds are provided in Fig. 6. The unaffected base plate hardness is consistent for all welds in the range of 40–45 $HV_{0.1}$. Furthermore, a heat affected zone was created due to annihilation of dislocations formed during plate rolling. The HAZ was determined to be ~7 mm wide, with a hardness of 22–27 $HV_{0.1}$ in fully annealed state.

The fusion zone hardness of most welds were similar to the annealed base plate, i.e., in the range of 22–27 $HV_{0.1}$, irrespective of welding method. The high dilution of I-joint welding is the main reason for the low resulting hardness in the fusion zone [36]. The grain boundary (Hall–Petch) strengthening effect is minuscule in pure aluminium. Thus, grain refinement is not expected to reveal any significant impact on the final hardness.

The examined welds have a highly varying porosity content, as shown in Fig. 5. Voids can influence the local load bearing capacity negatively. The densest welds were GMAW Al-ref and GTAW Al-ref and Ti and Ti-TiB_2. These samples exhibited consistent hardness values due to lower probability of interference with voids. Conversely, GMAW Ti, TiC, and Ti-TiC and GTAW TiC showed a varying hardness profile, with dips in areas close to a (underlying) pore.

Particle strengthening can be a significant hardness contributor in aluminium welding [11]. The particle contribution is dependent on particle size, amount, and distribution. The particle concentration of the weld is relatively low when considering dilution (< 0.5 wt.%), implying a modest strength contribution of the added particles. Furthermore, micron-sized Ti and TiB_2 particles are too large to interfere with dislocations; hence, their contribution to the final hardness is insignificant, which is seen in Fig. 6. TiC is nanosized and therefore has the potential to enhance the strength and hardness of the weld metal. However, a TiC-reinforcing effect is not seen for GTAW. The TiC particles survived the weld

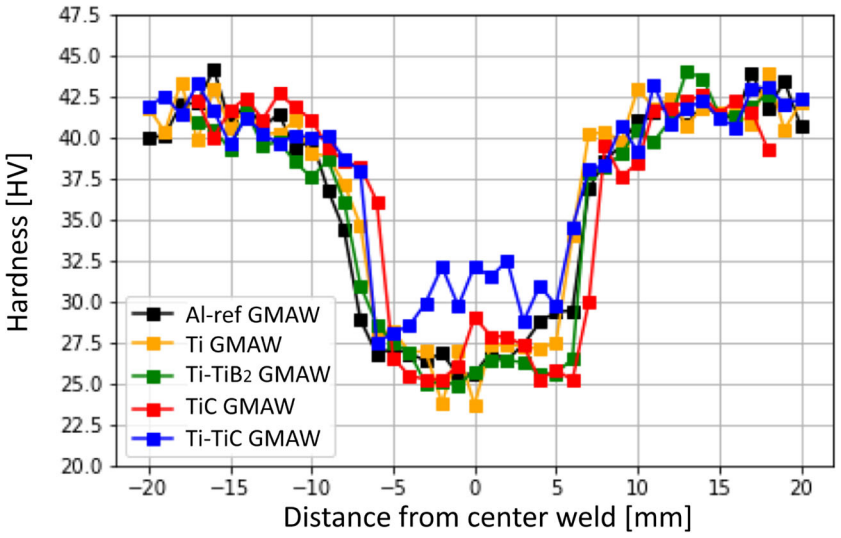

(a) GMAW

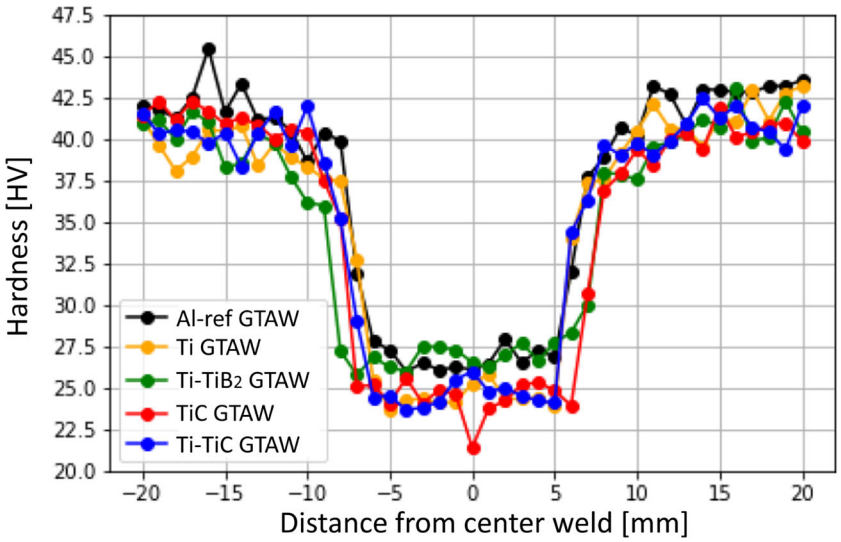

(b) GTAW

Fig. 6 Hardness profiles of all produced welds

heat cycle, but was observed in restricted areas of the weld as shown in Fig. 4f. The poor distribution of nanoparticles resulted in a low final hardness of the weld. The TiC GMAW weld exhibited a varying hardness curve, possibly due to an uneven distribution of TiC to the grain boundaries. One individual point at the weld centerline is among the highest values measured (29 $HV_{0.1}$), showing the potential of TiC. The GMAW Ti-TiC weld performed significantly better compared to all other welds. As TiC particles were situation on grain boundaries, the most fine grained material will have the most interactions with dislocations. However, further work should aim to incorporate the particles intragranularly, i.e., achieve wetting between TiC and aluminium [37].

4 Conclusions

This work has examined the effect of incorporating aluminium grain refiners to the filler wire by metal screw extrusion on microstructure and properties. A compound Ti–TiC addition to the filler wire provided the most potent grain refinement, possibly due to the formation of Al_3Ti intermetallics and a sufficiently large constitutional undercooled zone in GMAW. The welding method utilised has a strong effect on the final microstructure due to the thermal history of the filler wire. GTAW was unable to fully dissolve primary Ti particles, thus providing lower constitutional undercooling and less potent nucleation points. The use of metal screw

extrusion to manufacture tailored particle-reinforced filler wires is promising as to reduce the grain size and suppress the cracking susceptibility of non-weldable alloys.

Acknowledgements This publication has been funded by the SFI PhysMet (Centre for Research-based Innovation, 309584). The authors gratefully acknowledge the financial support from the Research Council of Norway and the partners of the SFI PhysMet.

Author Contributions K.M. Kirkbakk: formal analysis, investigation, methodology, visualisation, writing—review and editing. N. Marhaug: investigation, methodology, writing—review and editing. G. Kvam-Langelandsvik: investigation, methodology, visualisation, conceptualization, supervision, writing—original draft, writing—review and editing. J.C. Werenskiold: investigation, methodology, resources, conceptualization, supervision, writing—original draft, writing—review and editing.

Funding Open access funding provided by SINTEF. This work was supported by the SFI PhysMet (Centre for Research-based Innovation, 309584).

Data Availability Data and material can be provided upon request.

Code Availability Not applicable

Declarations

Competing interests The authors declare no competing interests.

References

1. Kou S (2003) Welding metallurgy. New Jersey, USA 431:223–225
2. Lippold JC (2014) Welding metallurgy and weldability (John Wiley & Sons)
3. Eurocode 9 (2007) Design of aluminium structures. Standard, European Committee for Standardization, Brussels, BE
4. Langelandsvik G, Akselsen OM, Furu T, Roven HJ (2021) Review of aluminum alloy development for wire arc additive manufacturing. Materials 14:5370. https://doi.org/10.3390/ma14185370
5. Ram, G. J., Mitra, T., Shankar, V. & Sundaresan, S. Microstructural refinement through inoculation of type 7020 Al–Zn–Mg alloy welds and its effect on hot cracking and tensile properties. Journal of Materials Processing Technology 142:174–181. https://doi.org/10.1016/S0924-0136(03)00574-0
6. Ram, G. J., Mitra T, Raju M, Sundaresan S (2000) Use of inoculants to refine weld solidification structure and improve weldability in type 2090 Al–Li alloy. Mater Scie Eng A 276:48–57. https://doi.org/10.1016/S0921-5093(99)00515-8
7. Schempp P, Rethmeier M (2015) Understanding grain refinement in aluminium welding. Welding in the World 59:767–784. https://doi.org/10.1007/s40194-015-0251-2
8. Cheng Y et al (2022) Studies on microstructure and properties of TiB_2-Al_3Ti ceramic particles reinforced spray-formed 7055 aluminum alloy fusion welded joints. J Mater Res Technol. https://doi.org/10.1016/j.jmrt.2022.05.116
9. Huang T et al (2021) Appropriate amount of TiB_2 particles causes the ductile fracture of the un-weldable spray-formed 7055 aluminium alloy TIG-welded joint. Mater Res Express 8:096512 https://doi.org/10.1088/2053-1591/ac2194
10. Fattahi M et al (2015) Effect of TiC nanoparticles on the microstructure and mechanical properties of gas tungsten arc welded aluminum joints. J Mater Process Technol 217:21–29. https://doi.org/10.1016/j.jmatprotec.2014.10.023
11. Sokoluk M, Cao C, Pan S, Li X (2019) Nanoparticle-enabled phase control for arc welding of unweldable aluminum alloy 7075. Nature Communications 10:1–8. https://doi.org/10.1038/s41467-018-07989-y
12. Ramanathan A, Krishnan PK, Muraliraja R (2019) A review on the production of metal matrix composites through stir casting–furnace design, properties, challenges, and research opportunities. J Manuf Process 42:213–245. https://doi.org/10.1016/j.jmapro.2019.04.017
13. Babu NK et al (2012) Influence of titanium–boron additions on grain refinement of AA6082 gas tungsten arc welds. Materials & Design 40:467–475. https://doi.org/10.1016/j.matdes.2012.03.056
14. Langelandsvik G et al (2020) Development of Al-Tic wire feedstock for additive manufacturing by metal screw extrusion. Metals 10:1485. https://doi.org/10.3390/met10111485
15. Mathers G (2002) The welding of aluminium and its alloys (Elsevier, 2002)
16. ASTM E112-13(2021) Standard test methods for determining average grain size. Standard, American Society for Testing and Materials, West Conshohocken, PA, USA (2021)
17. ISO 6507-1 (2018) Vickers hardness test. Part 1: Test method. Standard, International Organization for Standardization, Geneva, CH
18. Mitrašinović, A. & Hernández, F. R. Determination of the growth restriction factor and grain size for aluminum alloys by a quasi-binary equivalent method. Materials Science and Engineering: A **540**, 63–69 (2012). https://doi.org/10.1016/j.msea.2012.01.072
19. Schempp P, Cross CE, Schwenk C, Rethmeier M (2012) Influence of Ti and B additions on grain size and weldability of aluminium alloy 6082. Welding in the World 56:95–104. https://doi.org/10.1007/BF03321385
20. Kirkbakk KM (2022) Aluminum weld metal inoculation by TiTIB-textsubscript2TIC additions to screw extruded filler wires. Master's thesis, NTNU. https://hdl.handle.net/11250/3026009
21. Zhang M-X, Kelly P M, Easton MA, Taylor JA (2005) Crystallographic study of grain refinement in aluminum alloys using the edge-to-edge matching model. Acta Materialia 53:1427–1438. https://doi.org/10.1016/j.actamat.2004.11.037
22. Yu L, Liu X (2007) Ti transition zone on the interface between TiC and aluminum melt and its influence on melt viscosity. J Mater Process Technol 182:519–524. https://doi.org/10.1016/j.jmatprotec.2006.09.011
23. Mousavi M, Cross C, Grong Ø (1999) Effect of scandium and titanium–boron on grain refinement and hot cracking of aluminium alloy 7108. Science and Technology of Welding and Joining 4:381–388. https://doi.org/10.1179/136217199101538030
24. Mohanty P, Gruzleski J (1995) Mechanism of grain refinement in aluminium. Acta Metallurgica et Materialia 43:2001–2012. https://doi.org/10.1016/0956-7151(94)00405-7

25. Wang K et al (2016) Nanoparticle-inhibited growth of primary aluminum in Al–10Si alloys. Acta Materialia 103:252–263. https://doi.org/10.1016/j.actamat.2015.10.005
26. Greer A, Bunn A, Tronche A, Evans P, Bristow D (2000) Modelling of inoculation of metallic melts: application to grain refinement of aluminium by Al–Ti–B. Acta Materialia 48:2823–2835. https://doi.org/10.1016/S1359-6454(00)00094-X
27. Dvornak M, Frost R, Olson D (1991) Influence of solidification kinetics on aluminum weld grain refinement. Welding Journal 70:271s–276s
28. Langelandsvik G, Eriksson M, Akselsen OM, Roven HJ (2022) Wire arc additive manufacturing of AA5183 with TiC nanoparticles. The International Journal of Advanced Manufacturing Technology119:1047–1058. https://doi.org/10.1007/s00170-021-08287-6
29. Murphy AB (2011) A self-consistent three-dimensional model of the arc, electrode and weld pool in gas–metal arc welding. J Phys D: Appl Phys 44:194009. https://doi.org/10.1088/0022-3727/44/19/194009
30. Kah P, Latifi H, Suoranta R, Martikainen J, Pirinen M (2014) Usability of arc types in industrial welding. Int J Mech Mater Eng 9:1–12. https://doi.org/10.1186/s40712-014-0015-6
31. Han Y et al (2020) Numerical simulation of arc and droplet behaviors in TIG-MIG hybrid welding. Materials 13:4520. https://doi.org/10.3390/ma13204520
32. Fu R et al (2021) Hot-wire arc additive manufacturing of aluminum alloy with reduced porosity and high deposition rate. Materials & Design 199:109370. https://doi.org/10.1016/j.matdes.2020.109370
33. Yan B, Gao HM, Lin W, Neng C et al (2010) Influence of plasma-MIG welding parameters on aluminum weld porosity by orthogonal test. Transactions of Nonferrous Metals Society of China 20:1392–1396. https://doi.org/10.1016/S1003-6326(09)60310-1
34. Ransley C (1948) The solubility of hydrogen in liquid and solid aluminium. Journal of the Institute of Metals 74:599–620
35. Kusoglu IM et al (2022) Microstructure and corrosion properties of PBF-LB produced carbide nanoparticles additivated AlSi10Mg parts. Procedia CIRP 111:10–13. https://doi.org/10.1016/j.procir.2022.08.046
36. Mousavi M, Cross C, Grong Ø, Hval M (1997) Controlling weld metal dilution for optimised weld performance in aluminium. Science and Technology of Welding and Joining 2:275–278. https://doi.org/10.1179/stw.1997.2.6.275
37. Liu W, Cao C, Xu J, Wang X, Li X (2016) Molten salt assisted solidification nanoprocessing of Al-TiC nanocomposites. Materials Letters **185**, 392–395. https://doi.org/10.1016/j.matlet.2016.09.023